NANO LETTERS

2007
Vol. 7, No. 8
2529−2534

High-Performance Dual-Action Polymer–TiO_2 Nanocomposite Films via Melting Processing

Anna Kubacka,[†] Cristina Serrano,[†,‡] Manuel Ferrer,*[,†] Heinrich LUnsdorf,[§] Piotr Bielecki,[§] María Luisa Cerrada,[‡] Marta Fernández-García,[‡] and Marcos Fernández-García*[,†]

Instituto de Catálisis y Petroleoquímica, CSIC, C/Marie Curie 2, 28049 Madrid, Spain, Instituto de Ciencia y Tecnología de Polímeros, CSIC, C/Juan de la Cierva 3, 28006 Madrid, Spain, and Helmholtz-Zentrum fur Infektionsforschung, Inhoffenstrasse 7, 38124 Braunschweig, Germany

Received April 23, 2007

ABSTRACT

The incorporation of TiO_2 nanoparticles into (ethylene–vinyl alcohol)-based food packaging copolymers affords an opportunity to synthesize polymer-based nanocomposite materials with novel and powerful biocidal and photodegradability properties, resulting in the production of an advanced, environmentally friendly system prepared using a cost-effective synthesis method via a simple melt compounding without the need of a coupling agent incorporation. The presented materials display an unprecedented performance in the killing of both Gram positive and negative bacteria without the necessity of being release to the media and an easy degradation under sunlight which favorably competes with biodegradation procedures.

High-performance composite materials are actively being sought in the quest to add novel properties to polymer-based systems used in the industry.[1] In this field, modification of a polymeric matrix to prevent growth or reduce adhesion of detrimental microorganisms is a highly desired objective. Hence, there is a significant interest in the development of antimicrobial biomaterials for application in the health and biomedical device, food, and personal hygiene industries. Those agents need to combine desirable attributes such as potent bactericidal and fungicidal efficiency, environmental safety, low toxicity, and easy/cost-effective fabrication. Three broad classes of materials are currently used for rendering antimicrobial properties: (a) synthetic macromolecules/polymers that mimic naturally occurring bactericidal molecules/peptides; (b) microbe-repelling antiadherence polymers; (c) inorganic/organic materials with a slow releasing of biocides such as heavy metals or oxides (particularly based on silver), small molecule biocides, halogen species, or nitric oxide.[1,2] Options a and b are usually cost ineffective for a general application while option c requires the release of an agent potentially toxic for humans and the environment and typically with weaknesses in the attack to a certain class (Gram negative or positive bacteria, virus, and fungus) or to specific microorganisms.

TiO_2 is an inert, nontoxic, and cheap material which use does not require any release from a nanocomposite material but has potential activity against all kinds of microbes. Additionally, TiO_2 is able to eliminate (within an extended period of time) dead cells rendering CO_2, opening in this way a path for the autoregeneration of the system.[1a,3] All these together properties lead to a safer, cost-effective technology of universal application as an alternative to current inorganic- and organic-based biocidal agents. The presence of TiO_2 in a polymer matrix also provides a way to solve the general problem of disposal after completion of lifetime using an environmental friendly procedure. To add these two properties rendering advanced, dual-action polymers, the use of a light source is required. Under light excitation with energy above the TiO_2 band gap (3.2 eV), the formation of energy-rich electron−hole pairs is produced. Once at the surface of the material, such charge carriers are able to interact with the neighboring media and infer the necessary physicochemical characteristics to the nanocomposite to be both biocidal and degradable.[4] TiO_2-containing polymer-based nanocomposites have been previously studied, but a complete lack of reports aiming to work with a nanoparticulated oxide (particle size below 10 nm) and to

* Corresponding authors. E-mail: mfg@icp.csic.es (M.F.G.) mferrer@icp.csic.es (M.F.).
[†] Instituto de Catálisis y Petroleoquímica, CSIC, C/Marie Curie 2.
[‡] Instituto de Ciencia y Tecnología de Polímeros, CSIC, C/Juan de la Cierva 3.
[§] Helmholtz-Zentrum fur Infektionsforschung.

10.1021/nl0709569 CCC: $37.00
Published on Web 07/11/2007

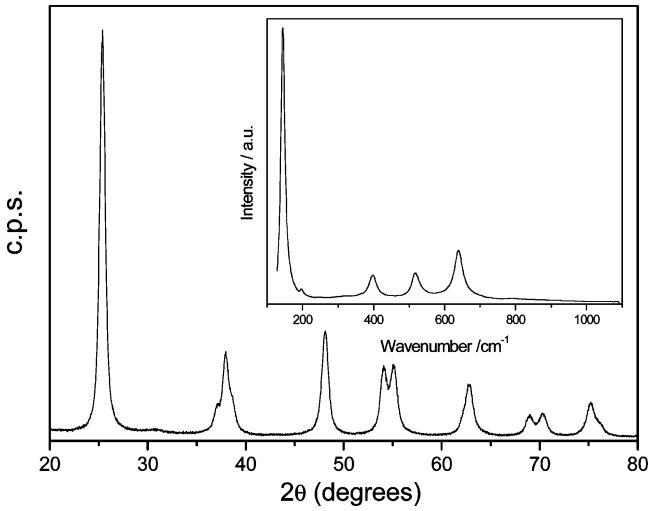

Figure 1. X-ray diffraction pattern and Raman spectrum of the TiO_2 component.

combine these two properties in a polymer with industrial aim within the food packaging area is noticed. Additionally, very few attempts have attained an acceptable dispersion of the inorganic component in a polymer matrix and, consequently, the introduction of an adequate amount to ensure the homogeneous presence of the biocidal agent in the whole material.[1]

In this Letter we describe ethylene−vinyl alcohol copolymer (EVOH)−TiO_2 nanoparticle composites for their application in the food packing industry,[1a] having potent long-lasting antimicrobial activity toward both Gram negative and positive bacteria and easy photodegradability with the help of a renewable source such as the sun. The embedded TiO_2 nanoparticles were previously prepared by a microemulsion method and calcined at 500 °C. Figure 1 displays the X-ray diffraction (XRD) and Raman spectra of this component, which showed an anatase structure with a BET area of ca. 104 $m^2\ g^{-1}$ and a primary particle size of ca. 9 nm. As detailed elsewhere, a narrow size distribution (standard deviation ±2 nm) and TiO_2 nanoparticles displaying an elongated shape along the {001} axis and mainly presenting (101) and (100) surface terminations were obtained with this preparation method.[5] A straightforward method was devised to introduce different contents of the inorganic solid into the polymeric matrix; after ultrasonic dispersion of TiO_2, the nanocomposites were prepared through a melt processing without incorporation of coupling agents in a shear mixer prototype at 195 °C/60 rpm for 5 min. After the components were blended, film specimens (ca. 200 μm) were obtained by compressing molding in a Collin press between hot plates at 210 °C at 1.5 MPa for 5 min. A quench from melt to room temperature (RT) was applied to the films with a 0.5, 2, and 5 wt % of TiO_2. As judged by the invariance of XRD/Raman peak widths and positions (at least in the 2 and 5 wt % samples, where detection of peaks was possible), no change in the oxide component primary particle morphology (size/shape) is detected through the preparation procedure (see Supporting Information Table S1).

Scanning electron microscopy (SEM) was applied to establish the homogeneity of the nanocomposite materials. Figure 2 exemplifies the high degree of dispersion of the oxide nanoparticles within the polymeric matrix; absence of detectable inorganic domains across the film is noticed up to a 2 wt % (micrographs b and c), while few agglomerates with a 2−3 μm characteristic size are detected in certain areas of the 5 wt % sample (micrograph d). The moderate hydrophilic nature of the EVOH component helps in obtaining this result, although there is an evident tendency of the TiO_2 nanoparticles to interact with each other. This coalescence trend seems however limited by the good blending obtained through the melt processing applied here and is only observed in very few micrograph sections (less than 10%) for a loading around 5 wt %. If compared with previous

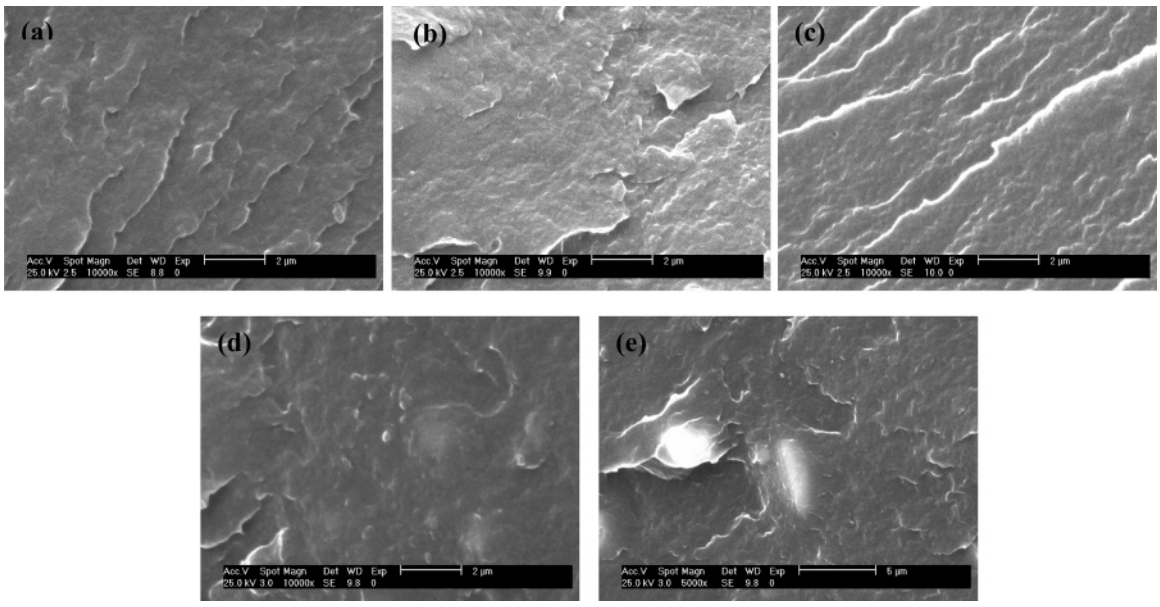

Figure 2. SEM micrographs showing cross-section views of (vacuum cleaved) EVOH−TiO_2 nanocomposites: (a) neat EVOH; (b) 0.5 wt % in TiO_2; (c) 2 wt % in TiO_2; (d) 5 wt % in TiO_2, and (e) small agglomerates at isolated zones found in the films with 5 wt % in TiO_2.

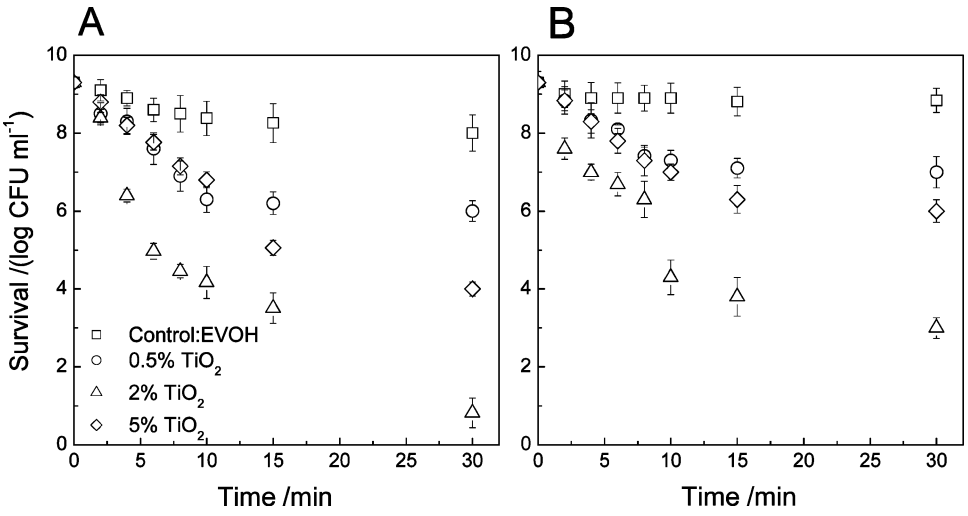

Figure 3. Process come-up time logarithmic reduction of microorganism population suspended in Luria−Bertani medium. Survival curves for *P. aeruginosa* (A) and *E. faecalis* (B) as a function of the irradiation time for EVOH−TiO_2 and control samples.

reports concerning TiO_2−polymer composites, the use of a nanostructured component with characteristic primary particle size below 10 nm clearly favors dispersion, allowing a significant improvement with respect to microsized or bulk oxides, particularly important for loadings above 1 wt %.[1c,6]

Antimicrobial properties of the resulting nanocomposite materials were tested in triplicate against Gram negative *Pseudomonas aeruginosa* and Gram positive (and facultative anaerobic) *Enterococcus faecalis* (see Supporting Information for details). Both microbes cause infections and serious illness, are widely present in the environment, and have a remarkable ability for biofilm formation.[7] *P. aeruginosa* is also known as one of the most drug and vaccine-resistant microorganism. Here we use antibiotic-resistant and clinically isolated strains, magnifying the interest of the result. Obviously, an antimicrobial component such as TiO_2 that actively disinfects surfaces in contact with potential microorganism sources must help in breaking infection loops. In our experiment, rather limited, sublethal radiation energy fluences (below 1 kJ m^{-2}) of a UV-A source (280 nm) were employed.[8] The control experiment using the parent copolymer matrix gives evidence of this; no significant log reduction was observed during the come-up time after the UV treatment using as substrate the single polymer component (1.16/1.05 log-reduction CFU mL^{-1}, Figure 3). For the initial, linear log-reduction parameter estimate fitting, a small slope of the log-survival was observed: 9.6(7) and 4.0(2) × 10^{-3} min^{-1} for *P. aeruginosa* and *E. faecalis*, respectively (Table 1). This fact demands 1.5/3.6 h of treatment for a 50% reduction if considering the initial rates reported in Table 1 while more than 20 h is estimated when using the whole curve displayed in Figure 3.

The presence of TiO_2 affects profoundly the biokilling potential of the nanocomposite material. No significant activity is detected in absence of UV light; however, when this was switched on, *P. aeruginosa* appeared as the most affected strain among the two studied (Figure 3A). After 10 min of treatment, 3.0, 5.1, and 2.5 log-reductions were observed, respectively, for the 0.5, 2, and 5 wt % materials.

Table 1. Cell Inactivation Initial Rates and Time for 50% Reduction Measured Using the EVOH−TiO_2 Composites (See Text for Details)

sample	initial rates/10^{-2} log reduction min^{-1} [a]	$T_{1/2}$/min
	P. aeruginosa	
control: EVOH	0.96(0.07)	
0.5 wt %	2.9(0.2)	40
2 wt %	7.5(0.7)	8.5
5 wt %	2.6(0.1)	22
	E. faecalis	
control: EVOH	0.4(0.2)	
0.5 wt %	2.1(0.3)	68
2 wt %	4.3(0.6)	14
5 wt %	2.3(0.3)	40

[a] Standard error in parentheses.

These values increasing up to 3.3, 8.5, and 5.3 by the end of the experiment (30 min), in the characteristic tailing region displayed after an extended period of UV treatment. As shown in Table 1, cell inactivation occurs initially (initial rates) up to about 8 times faster than that obtained for the control experiment measuring the effect of the UV light in the presence of the single polymer component. The final result is an optimum 8.5 log-reduction for the 2 wt % sample. Considering that this is obtained with a 2 × 10^{-2} mg mL^{-1} TiO_2 concentration, it can be concluded that our system displays an unprecedented power for *P. aeruginosa* destruction, well above the 5.4 log-reduction/1 h or the 3.5 log-reduction/40 min shown, respectively, by TiO_2 supported on Plexiglas or as a powder (Degussa P25).[9a,b] Also, comparison with reported results using Ag-based systems (commercial AgION coating stain steel 1.6 log-reduction/4 h;[9c] AgBr particles coating poly(vinylpyridine)-NPVP 4 log-reduction[2d]) or simple chemicals like glutaraldehyde, formaldehyde, H_2O_2, phenol, cupric ascorbate, or sodium hypochlorite (below 6 log-reduction/30 min)[2g] reinforces our conclusion; none of these biocidal agents displays comparable results in terms of efficiency or time response. To further stress this

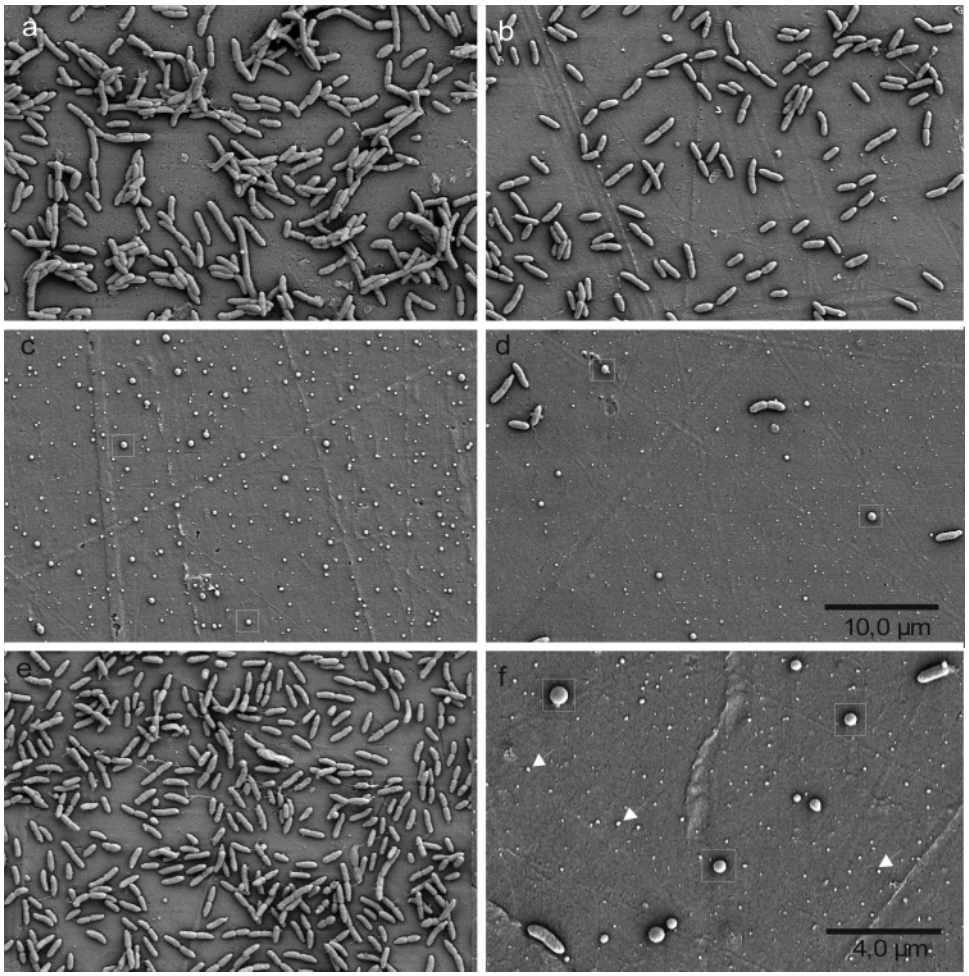

Figure 4. SEM images of the *P. aeruginosa* cells sited at the surface of the EVOH−TiO_2 nanocomposites in the presence and absence of UV light: (a) Survey view of biofilm adhesive growth of cells on a EVOH substratum but irradiated with UV (substratum control). (b) Cells grown after UV treatment in the presence of 0.5 wt % TiO_2. (c) Cells in the presence of 2 wt % TiO_2 and after UV irradiation. (d) After UV exposure and at 5 wt % TiO_2 content. (e) UV control, i.e., cells grown in the presence of 2 wt % TiO_2 but without UV irradiation. (f) Detailed view of *P. aeruginosa* cells after UV irradiation at 5 wt % TiO_2. Squared boxed particles (c, d, f) represent rounded forms of bacterial fragments/cells; arrows (f) indicate minimum spheroids as final cellular states of the experimental treatments.

comparison, we mention that an Ag dispersal to the media in the 50−1500 μg mL^{-1} interval (depending on the Ag−polymer nanocomposite system) is needed for a certainly much less effective response.[2d,9c] Long-term exposures to such concentrations may cause health problems in uncontrolled situations. We also note here that the interaction with the polymer is a must in order to get a large TiO_2 dispersion and to enhance its biocidal properties; if the oxide is used alone, a 8×10^{-1} (vs 2×10^{-2}) mg mL^{-1} concentration is needed to obtain a similar level of cell inactivation. This, despite the well-known fact that titania nanoparticles in suspension can be ingested by microorganisms by phagocytosis, causing rapid cellular damage in addition to that caused by photocatalysis.[2c,9e,f,10] Additionally, once oxide aggregation is detected in the composite material, e.g., around 5 wt %, a certain loss of biocidal activity is detected. The joint analysis of all these points leads to the conclusion that the maximization of both the available TiO_2 surface area and dispersion homogeneity within the polymer matrix are key features in optimizing biokilling activity in our nanocomposite materials.

The analysis of the biocidal properties of the nanocomposite material is completed with tests using the Gram positive cocci *E. faecalis*. Here, in the first 10 min we found a similar behavior to the one displayed in the case of *P. aeruginosa*: e.g., 2.0, 5.0, and 2.3 log-reduction values for the 0.5, 2, and 5 wt % samples, respectively (Figure 3B). The initial rates included in Table 1 are consistent with this similar behavior, showing a maximum (10 times faster than the control experiment), corresponding to the 2 wt % sample. The efficiency of the samples slows up toward the end of the experiment (characteristic tailing) but an optimum value of 6.3 log-reduction after 30 min of treatment was obtained with the 2 wt % sample. Accordingly, the $T_{1/2}$ data (Table 1) presented a somewhat inferior performance with respect to that shown for *P. aeruginosa*. Comparison with literature data in the case of *E. faecalis* is somewhat difficult due to the practical absence of previous reports. Nonetheless, a TiO_2−Ni composite coating was previously tested, showing a maximum 2 log-reduction in extended period of times.[11a] Other biocides used are simple chemicals (triclorosan present in styrene−acetate-based polymers showed a cell inactivation

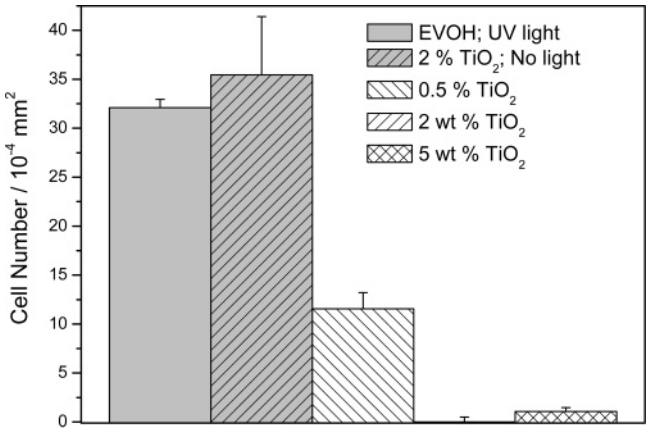

Figure 5. Impact of TiO_2 on *P. aeruginosa* cell number per mm^2 after treatment of the control and EVOH−TiO_2 composites in the presence and absence of UV light.

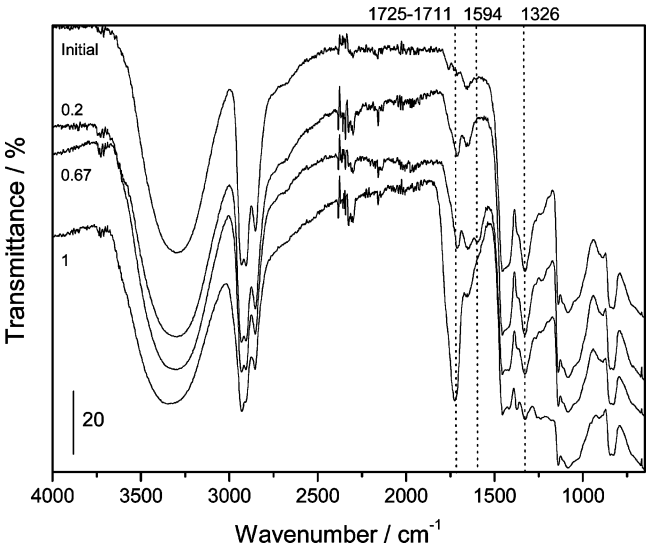

Figure 6. ATR-FTIR spectra of the nanocomposite containing 2 wt % of TiO_2 during an aging treatment under simulated sunlight for 2 months. Spectra showed slides at different cumulative exposure times up to the end of treatment (marked as 1 in the figure).

initial rate enhancement below 2 with respect to the polymer alone),[11b] UV-sensitive organometallic complexes leading to oxygen radical formation (3.5 log-reduction/4 h),[11c] or UV-treated Nylon (1.8 log-reduction/6 h).[11d] None of them approaches the performance here displayed by the 2 wt % sample. Again, we note that the maximum of activity parallels the dispersion of the TiO_2, being the nanocomposite with 2 wt % significantly superior to the parent oxide system. The occurrence of an optimum for a 2 wt % using both microorganisms suggests that limited differences between samples 2 and 5 wt % performance are mainly related to morphological aspects of the oxide component (the secondary particle size and dispersion within the polymer matrix of the oxide in the nanocomposite, as evidenced in Figure 2).

A SEM study of *P. aeruginosa* adhesion and biofilm formation was performed in order to further analyze the bactericidal properties of our nanocomposites and to translate the data depicted in Figure 3 and Table 1 in visual information. As can be observed in parts a and e of Figure 4 adhesion/interaction of bacteria to/with the polymer surface is certainly modified by the UV light and/or by the presence of TiO_2. In the absence of the oxide but actual UV-treatment cells appear mainly aggregated by lateral contact of two or more cells, whereas in the presence of actual 2 wt % TiO_2 but without UV irradiation bacteria appear mainly nonaggregated, evenly distributed over the substratum surface, with only seldom lateral contacts. Maybe these differences are caused or influenced by different physiological and/or signaling states of *P. aeruginosa* cells in both experiments, in turn related or somewhat affected with differences in the substrata surface chemistry, i.e., polymer versus oxide. In any case, the stronger aggregation behavior displayed in absence of TiO_2 but under UV light does not however appear to affect significantly the total number of cells present at the surface of the material. Numerical analysis of the biofilm bacterial densities (given as number of cells per square millimeter) is presented in Figure 5 and confirms the qualitative impression evolving from Figure 4. Illumination of the nanocomposite systems using similar experimental conditions as in Figure 3 makes, as expected, a dramatic effect on cell viability. While a significant decrease in survival probability is detected for the 0.5 wt % composite, a complete or near-complete killing is observed for the other two composites having larger TiO_2 loadings (Figures 4 and 5). Dead cells with rounded shapes but mostly cell debris can be observed in panels c and d of Figure 4. Taking into account data reported on *P. aeruginosa*,[12] rounded shapes would indicate the presence of lysed cells (0.54 ± 0.10 μm diameter; $N = 142$) with a restricted number of breaks in their cell walls. In a subsequent step, viability of the cell is fully lost by further attack of TiO_2-derived radicals, just leaving cell debris with a characteristic diameter of 280 ± 70 nm ($N = 574$) at the surface of the nanocomposite material (Figure 4c,d). Note that this process does not produce significant amounts of flattened ghosts and similar bacterial residues but only rather size-limited debris (well below characteristic dimensions of the bacteria), allowing an optimum and continuous use of the nanocomposite material and limiting a potential lost of efficiency by excessive accumulation of cellular debris at the surface. Thus, these data provide conclusive evidence that TiO_2 presence not only affects cell viability but also bacteria aggregation and biofilm formation.

Photodegradability using a renewable energy source and, consequently, the production of environmentally friendly polymeric materials is another plus expected from TiO_2 addition to the EVOH matrix. This process was followed here using infrared spectroscopy. Figure 6 depicts the cumulative effect of light irradiation up to 2 months of simulated sunlight exposure in the attenuated total reflection Fourier transform infrared (ATR-FTIR) spectrum of the 2 wt % sample. While UV light is known to have a rather limited aging effect on EVOH polymers,[13a] the progressive degradation of the polymer matrix is evidenced in the case of the TiO_2-containing nanocomposites by the spectra displayed in the figure. At the initial part of the treatment, only small bands at 1711 and 1594 cm^{-1} can be discerned

as new features. The first is associated with the progressive presence of carbonyl moieties (C−O stretch) while the second is related to changes in the bending O−H mode. Both bands provide evidence of the TiO_2 presence in the OH-rich, hydrophilic zones of the polymer where the degradation starts by oxidation of the vinyl alcohol moieties. The treatment effect accelerates after 2/3 of the time period scanned. The corresponding FTIR spectra show important alterations in the O−H stretch (3500−3000 cm^{-1}) and bending/deformation (1590/1390 cm^{-1}) modes with a parallel increase in the 1725−1710 cm^{-1} band intensity related, as mentioned, to the appearance of carbonyl groups.[13] These observations evidence the strong degradation of the hydrophilic part of the polymer attained in the last third of the treatment, with a parallel and modest modification of the ethylene groups, as suggested by small changes in the 2900−2800 (symmetric/asymmetric CH_2 stretching modes) and 1400 (bending CH_2 mode) cm^{-1} zones. The speed of the TiO_2-assisted polymeric matrix degradation reported in Figure 6 is clearly competitive with that observed by using biodegradation procedures.[13b,g]

To briefly conclude, we have described the preparation of an organo−inorganic hybrid nanocomposite via a straightforward and cost-effective approach allowing the incorporation of nanoscale TiO_2 within a polymeric EVOH matrix, in significant amounts, well above 1 wt %, with respect to previous reports.[1,6] As demonstrated by SEM, the important dispersion of the oxide component is a key property to obtain enhanced antimicrobial properties relating to cell but also biofilm viability in the case of both Gram positive and negative micro-organisms. Notice that the current nanocomposites outperform the Ag-based and all known biocide agents and do not require their release in the media. Presence of TiO_2 in the nanocomposite material also opens a way to obtain environmentally friendly materials, having enhanced degradation properties with respect to current alternatives (biodegradation) while using sunlight as the energy source of the process.

Acknowledgment. Dr. A. Kubacka and Ms C. Serrano thank the CSIC for I3P postdoctoral and doctoral grants. We thank Britta Scheithauer for providing the *E. faecalis* strain. This work was supported by the CSIC under the projects PIF200580F0101 and PIF200560F0103.

Supporting Information Available: Descriptions of experimental details including sample preparation, strains and bacterial cultures, photochemical viability assays, visualization and quantification of *P. aeruginosa* and *E. faecalis* on nanocomposites, and other techniques and a table containing XRD and Raman results on polymer−TiO_2 nanocomposites. This material is available free of charge via the Internet at http://pubs.acs.org.

References

(1) (a) Appendini, P.; Hotchkiss, J. N. *Innovative Food Sci. Emerging Technol.* **2002**, *3*, 113−126. (b) Devlieghere, F.; Vermein, L.; Debevere, J. *Int. Dairy J.* **2004**, *14*, 273−285. (c) Brody, A. L. *Food Technol.* **2003**, *57*, 52−54.

(2) (a) Tang, H.; Doerksen, S.; Tew, G. N. *Chem. Commun.* **2005**, *12*, 1537−153. (b) Gilbert, B.; Markova, N.; Cossement, D.; Gouttebaron, R.; Jeromec, C. *Langmuir* **2006**, *22*, 255−262. (c) Brayner, R.; Ferrari-Iliou, R.; Brivois, N.; Djediat, S.; Benedetti, M. F.; Fievet, F. *Nano Lett.* **2006**, *6*, 866−870. (d) Sambhry, V.; Mecbridge, M.; Peterson, B. R.; Sen, A. *J. Am. Chem. Soc.* **2006**, *128*, 9796−9808. (e) Dizman, B.; Elasri, M. O.; Mathias, L. *Biomacromolecules* **2005**, *6*, 514−520. (f) Iconomopoulu, S. M.; Voyiatzias, G. A. *J. Controlled Release* **2003**, *103*, 451−464. (g) Sagripanti, J. C.; Bnonifacio, A. *J. AOAC Int.* **2000**, *83*, 1415−1422. (h) Chen, Y.; Worley, S. D.; Kim, J.; Wei, T. Y.; Santiago, J. I.; Williams, J. F.; Sun, G. *Ind. Eng. Chem. Res.* **2003**, *42*, 280−284. (i) Robbins, M. E.; Hopper, E. D.; Schoenfish, A. *Langmuir* **2004**, *20*, 10296−10302.

(3) (a) Jacob, W. A.; Maness, P. C.; Wolfrum, E. J.; Blake, D. M.; Fennel, J. A. *Environ. Sci. Technol.* **1998**, *32*, 2650−2653. (b) Brook, L. A.; Evans, P.; Foster, H. A.; Pemble, M. E.; Steeler, A.; Yates, H. M. *J. Photochem. Photobiol., A* **2004**, *187*, 53−63.

(4) (a) Dietbol, U. *Surf. Sci. Rep.* **2003**, *48*, 53−229. (b) Fernández-García, M.; Martínez-Arias, A.; Hanson, J. C.; Rodríguez, J. A. *Chem. Rev.* **2004**, *104*, 4063−4104. (c) Carp, O.; Huisan, C. L.; Reller, A. *Prog. Solid State Chem.* **2004**, *32*, 33−177. (d) Hoffmann, M. R.; Martin, S. T.; Choi, W.; Bahemann, D. W. *Chem. Rev.* **1995**, *95*, 69−96.

(5) (a) Fernández-García, M.; Wang, X.; Belver, C.; Hanson, J. C.; Rodríguez, J. A. *J. Phys. Chem. C* **2007**, *111*, *674−682.* (b) Fuerte, A.; Hernández-Alonso, M. D.; Maira, A. J.; Martínez-Arias, A.; Fernández-García, M.; Conesa, J. C.; Soria, J.; Munuera, G. *J. Catal.* **2002**, *212*, 1−9.

(6) (a) Sanchez, C.; Julian, B.; Belleville, P.; Popall, M. *J. Mater. Chem.* **2005**, *15*, 3559−3592. (b) Wang, Z.; Li, G.; Pen, H.; Zhang, Z.; Wang, X. *J. Mater. Sci.* **2003**, *40*, 6433−6438.

(7) Tolker-Nielsen, T.; Molins, S. *Pseudomonas*; Kluwer-Plenum: New York, 2004; pp 547−571.

(8) Noakes, C. J.; Fletcher, L. A.; Beggs, C. B.; Sleigh, P. A.; Kerr, K. G. *Aerosol Sci.* **2004**, *35*, 489−507.

(9) (a) Kuhn, K. P.; Chaberny, I. F.; Massholder, K.; Stickler, M.; Benz, V. W.; Sonnatg, H.-G.; Erdinger, L. *Chemosphere* **2003**, *53*, 71−77. (b) Ibañez, J. A.; Litter, M. I.; Pizarro, R. A. *J. Photochem. Photobiol., A* **2003**, *157*, 81−85. (c) Cowan, M. M.; Abshire, K. Z.; Houk, S. L.; Evans, S. M. *J. Ind. Microbiol. Biotechnol.* **2003**, *30*, 102−106. (d) Seven, O.; Dinder, B.; Aydemir, S.; Metin, D.; Ozinel, M. A.; Icli, S. *J. Photochem. Photobiol., A* **2004**, *165*, 103−107. (e) Amézaga-Madrid, P.; Nevárez-Moorillón, G. V.; Orrantia-Borunda, E.; Miki-Yoshida, M. *FEBS Microbiol. Lett.* **2002**, *211*, 183−188.

(10) (a) Huang, Z.; Maness, P. C.; Blake, D. M.; Wolfrum, E. J.; Smolinski, S. L.; Jacoby, W. A. *J. Photochem. Photobiol., A* **2000**, *130*, 163−169. (b) Sunada, K.; Watanabe, T.; Hashimoto, K. *J. Photochem. Photobiol., A* **2003**, *156*, 227−235.

(11) (a) Zhi-hong, Z.; Sakagami, Y.; Osaka, T. *Chem. Lett.* **1997**, *909−910.* (b) Chung, D.; Papadakis, S. E.; Yam, K. L. *Int. J. Food Sci. Technol.* **2003**, *38*, 165−169. (c) Villén, L.; Majón, F.; García-Resnadillo, D.; Orellana, G. *Appl. Catal. B* **2006**, *69*, 1−9. (d) Shearer, A. E. H.; Park, J. S.; Hoover, D. G.; Hayne, S. L. *Biotechnol. Bioeng.* **2000**, *67*, 141−146.

(12) Monden, K.; Ando, E.; Iida, M.; Kumon, H. *J. Infect. Chemother.* **2002**, *8*, 218−226.

(13) (a) Carlsson, D. J.; Chmela, S.; Wiles, D. M. *Polym. Degrad. Stab.* **1991**, *31*, 255−267. (b) Erlandsson, B.; Karlsson, S.; Albertsson, A.-C. *Acta Polym.* **1998**, *49*, 363−370. (c) Coleman, M. M.; Painter, P. C. *Prog. Polym. Sci.* **1995**, *20*, 1−9. (d) Socrates, G. *Infrared Characteristic group frequencies*; Wiley: Chichester, 1980. (e) Su, Z.; Zhao, Y.; Zhang, X.; Zhu, S.; Wang, D.; Wu, J.; Han, C. C.; Xu, D. *Macromolecules* **2004**, *37*, 3249−3256. (f) Folder, E.; Pokanzky, B. *J. Colloid Interface Sci.* **2005**, *283*, 79−86. (g) See: http://bpsweb.net/english/e-products.html.

NL0709569